

Theoretical prediction of energy release rate for interface crack initiation by thermal stress in environmental barrier coatings for ceramics

E Kawai¹, Y Umeno¹

¹ Institute of Industrial Science, The University of Tokyo, 4-6-1, Komaba Meguro-ku, Tokyo 153-8505, Japan
E-mail: kawai@ulab.iis.u-tokyo.ac.jp

Abstract. As weight reduction of turbines for aircraft engines is demanded to improve fuel consumption and curb emission of carbon dioxide, silicon carbide (SiC) fiber reinforced SiC matrix composites (SiC/SiC) are drawing enormous attention as high-pressure turbine materials. For preventing degradation of SiC/SiC, environmental barrier coatings (EBC) for ceramics are deposited on the composites. The purpose of this study is to establish theoretical guidelines for structural design which ensures the mechanical reliability of EBC. We conducted finite element method (FEM) analysis to calculate energy release rates (ERRs) for interface crack initiation due to thermal stress in EBC consisting of Si-based bond coat, Mullite and Ytterbium (Yb)-silicate layers on a SiC/SiC substrate. In the FEM analysis, the thickness of one EBC layer was changed from 25 μm to 200 μm while the thicknesses of the other layers were fixed at 25 μm , 50 μm and 100 μm . We compared ERRs obtained by the FEM analysis and a simple theory for interface crack in a single-layered structure where ERR is estimated as nominal strain energy in the coating layers multiplied by a constant factor (independent of layer thicknesses). We found that, unlike the case of single-layered structures, the multiplication factor is no longer a constant but is determined by the combination of consisting coating layer thicknesses.

1. Introduction

To improve fuel consumption and curb emission of carbon dioxide, the weight reduction of turbines for aircraft is demanded [1-3]. Silicon carbide (SiC) fiber reinforced SiC matrix composites (SiC/SiC) are attractive materials as high-pressure turbine materials because this composites have the superior heat resistance and the density of it is approximately one-third of Nickel-based super alloys which are used for turbine materials [4, 5].

At high temperature, SiC/SiC composites react with oxygen to form an oxide layer, which hinders degradation of SiC/SiC [6, 7]. However, under the high temperature and water vapor environments where high-pressure turbines are used, the oxide layer reacts with water vapor to form a volatile hydroxide layer [6, 7]. This leads to wall thinning or disappearance of the oxide layer and degradation of SiC/SiC. In order to maintain the property of SiC/SiC, development of environmental barrier coatings (EBC) for SiC/SiC is essential. EBC is fabricated by depositing several layers on a SiC/SiC substrate at high temperature and cooling it to room temperature. During the fabrication process, delamination cracks are initiated due to the thermal stress which occurs by the difference in coefficients of thermal expansion (CTEs) of the coating layers and the substrate. For sophisticated design to prevent the interface crack initiation, it is necessary to theoretically identify critical



thicknesses of the coating layers. The aim of this study is to establish theoretical guidelines for the condition of the coating layer thicknesses that ensures the mechanical reliability of EBC.

2. Theoretical framework of energy release rate for interface crack initiation in multi-layered structure

Assuming a biaxial stress state, the energy release rate (ERR) for interface crack initiation in single-layered isotropic elastic structure is evaluated by the following equation [8],

$$G = Z \frac{\sigma^2 h_{\text{film}}}{E_{\text{film}}}, \bar{E}_{\text{film}} = \frac{E_{\text{film}}}{1 - \nu_{\text{film}}^2}, \quad (1)$$

where G is ERR, Z is a dimensionless constant depending on the cracking pattern and elastic mismatch ($Z = 1.028$ for crack initiation at interface with vanishing elastic mismatch [8]). E_{film} , ν_{film} and h_{film} are Young's modulus, Poisson's ratio and thickness of the film, respectively. The thermal stress, σ , which occurs due to cooling from high temperature (T_h) to room temperature (T_r), is written as

$$\sigma = (\alpha_{\text{film}} - \alpha_{\text{sub}})(T_h - T_r) \frac{E_{\text{film}}}{1 - \nu_{\text{film}}^2}. \quad (2)$$

Note that α_{film} and α_{sub} are CTEs of the film and substrate, respectively.

To predict ERR for interface crack initiation in multi-layered structure, we regard the coating layers above the objective interface as one film and the other layers below the interface as a substrate. Then, ERR is given by

$$G = Z \sum_{i=1}^n \frac{\sigma_i^2 h_i}{E_i}, \bar{E}_i = \frac{E_i}{1 - \nu_i^2}. \quad (3)$$

Here, $i = 1, \dots, n$ indicate the layers of the objective structure. Note that Z in eq. (3) is no longer a constant determined by elastic properties of the components but depends on thicknesses of the coating layers and substrate because ERR should be governed by the 'effective' mismatch between the layers over and below the interface in question. To examine the significance of the dependence of Z on layer thicknesses, in Sec.3 we calculate ERR using numerical calculations to be compared with G_T , which is calculated assuming Z is a constant ($Z = Z_T \equiv 1.028$).

3. Analytical procedure

The thermal stress finite element method (FEM: ABAQUS, ver6.14.5) analysis was conducted to calculate ERR (G_F) for each interface crack initiation in multi-layered structure and consider the dependence of Z on the layer thicknesses by comparing G_F and ERR obtained by eq. (3) with $Z = Z_T \equiv 1.028$ (G_T). The temperature difference upon cooling ($\Delta T = T_h - T_r$) was 1375 K. Figure 1 shows the FEM analysis model and boundary conditions. The axisymmetric model is adopted for EBC consisting of Yb-silicate (YbS), Mullite (Mu) and Si-based bond coat (BC) layers on a SiC/SiC substrate. All material were treated as isotropic elastic materials. In this paper, we refrain from disclosing the material properties. The region near the interfaces (YbS/Mu, Mu/BC and BC/(SiC/SiC)), where the stress concentration is expected, was divided into a finer mesh. In this analysis, the thickness of one layer in EBC was changed from 25 μm to 200 μm while the thicknesses of the other layers were fixed at 25 μm (Type A), 50 μm (Type B) and 100 μm (Type C). The displacement constraint in the y direction was imposed on the bottom end of the model. It was assumed that the interface crack (length: 900 μm) was initiated from the right side of the model.

G_F was obtained by

$$G_F = - \frac{\Pi_C - \Pi_{\text{NC}}}{\Delta A}, \quad (4)$$

where Π_C and Π_{NC} are nominal strain energies of the FEM models with and without crack, respectively, and ΔA is crack propagation area.

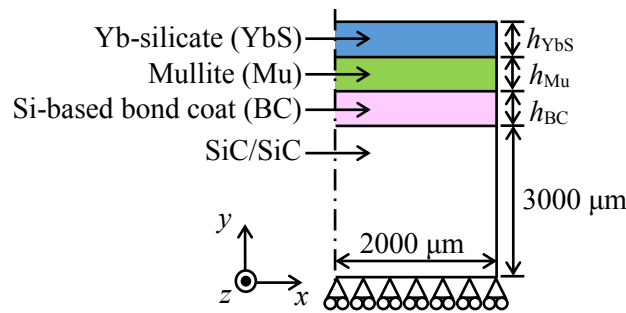


Fig. 1 Schematic illustration of FEM analysis model and boundary conditions.

4. Results and discussion

4.1. Theoretical prediction of ERRs for interface crack initiation in EBC

4.1.1. *Si-based bond coat/(SiC/SiC) substrate interface.* Figure 2 (a) shows the ratio of factor Z_T/Z determined by G_T/G_F for BC/(SiC/SiC) interface - thickness of the layers (h_i) relationship of Type A. As shown in Fig. 2 (a), Z_T/Z was changed by increasing the thickness of the layers. The relationships between Z_T/Z and h_i are given by

$$\frac{Z_T}{Z} = -1.00 \times 10^{-4} h_{YbS}^2 + 0.0327 h_{YbS} + 5.72, \quad (5)$$

$$\frac{Z_T}{Z} = -5.00 \times 10^{-4} h_{Mu}^2 + 0.135 h_{Mu} + 3.41, \quad (6)$$

$$\frac{Z_T}{Z} = 2.00 \times 10^{-4} h_{BC}^2 - 0.0506 h_{BC} + 6.44. \quad (7)$$

Here, h_{YbS} , h_{Mu} and h_{BC} are thicknesses of YbS, Mu and BC layers, respectively.

Figures 2 (b) and (c) show the Z_T/Z - h_i relationships of Type B and Type C, respectively. In both cases, Z_T/Z increases with the increase of h_{YbS} and h_{Mu} while it decreases with increasing h_{BC} . The relationships between Z_T/Z and h_i of these types are written as follows:

Type B

$$\frac{Z_T}{Z} = -3.00 \times 10^{-4} h_{YbS}^2 + 0.111 h_{YbS} + 1.63, \quad (8)$$

$$\frac{Z_T}{Z} = -2.00 \times 10^{-4} h_{Mu}^2 + 0.0940 h_{Mu} + 2.30, \quad (9)$$

$$\frac{Z_T}{Z} = 3.00 \times 10^{-4} h_{BC}^2 - 0.0784 h_{BC} + 9.63, \quad 50 \leq h_{BC} \leq 200 \quad (10)$$

Type C

$$\frac{Z_T}{Z} = -4.00 \times 10^{-5} h_{YbS}^2 + 0.060 h_{YbS} + 1.57, \quad (11)$$

$$\frac{Z_T}{Z} = -8.00 \times 10^{-5} h_{Mu}^2 + 0.0449 h_{Mu} + 3.42, \quad (12)$$

$$\frac{Z_T}{Z} = 2.00 \times 10^{-3} h_{BC}^2 - 0.628 h_{BC} + 52.8, \quad 50 \leq h_{BC} \leq 200 \quad (13)$$

Clearly, Z_T/Z - h_i relationship is determined by the combination of the film thicknesses, meaning that the theoretical prediction of ERR for BC/(SiC/SiC) interface crack initiation in EBC is described as

$$G_{BC/(SiC/SiC)} = Z_{BC/(SiC/SiC)}(h_{YbS}, h_{Mu}, h_{BC}) \left(\frac{\sigma_{YbS}^2 h_{YbS}}{\bar{E}_{YbS}} + \frac{\sigma_{Mu}^2 h_{Mu}}{\bar{E}_{Mu}} + \frac{\sigma_{BC}^2 h_{BC}}{\bar{E}_{BC}} \right), \quad \bar{E}_i = \frac{E_i}{1 - \nu_i^2}, \quad i = YbS, Mu, BC. \quad (14)$$

Here, $Z_{BC/(SiC/SiC)}(h_{YbS}, h_{Mu}, h_{BC})$ is a factor dependent on the combination of the YbS, Mu and BC layers.

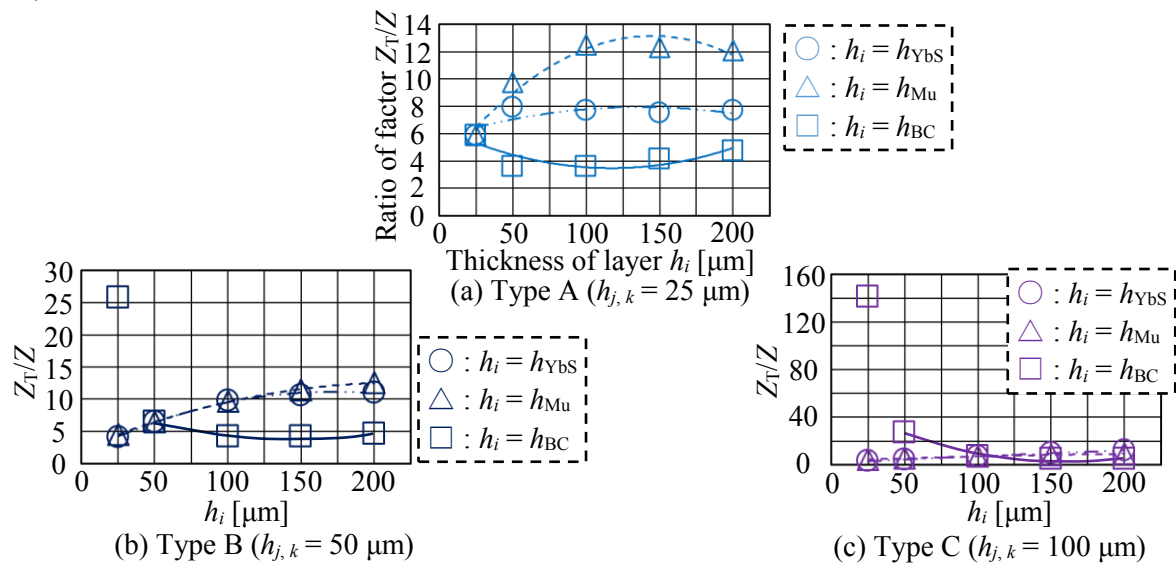


Fig. 2 Ratio of factor (Z_T/Z) for Si-based bond coat/(SiC/SiC) substrate interface – thickness of layers (h_i) relationships of (a) Type A, (b) Type B and (c) Type C.

4.1.2 *Mullite/Si-based bond coat interface.* Figure 3 shows the $Z_T/Z-h_i$ relationships for Mu/BC interface. In all types, Z_T/Z increases with the increase of h_{YbS} while it decreases with increasing h_{Mu} and h_{BC} . The relationships between Z_T/Z and h_i for Mu/BC interface are written as

Type A

$$\frac{Z_T}{Z} = 0.081h_{YbS} + 0.754, \quad (15)$$

$$\frac{Z_T}{Z} = 6.00 \times 10^{-5}h_{Mu}^2 - 0.0143h_{Mu} + 2.58, \quad (16)$$

$$\frac{Z_T}{Z} = 1.00 \times 10^{-4}h_{BC}^2 - 0.0316h_{BC} + 2.93, \quad (17)$$

Type B

$$\frac{Z_T}{Z} = 4.00 \times 10^{-5}h_{YbS}^2 + 0.0197h_{YbS} + 0.560, \quad (18)$$

$$\frac{Z_T}{Z} = 8.00 \times 10^{-5}h_{Mu}^2 - 0.0217h_{Mu} + 2.75, \quad (19)$$

$$\frac{Z_T}{Z} = 1.00 \times 10^{-4}h_{BC}^2 - 0.0380h_{BC} + 3.53, \quad (20)$$

Type C

$$\frac{Z_T}{Z} = 6.40 \times 10^{-3}h_{YbS} + 0.483, \quad (21)$$

$$\frac{Z_T}{Z} = 8.00 \times 10^{-5}h_{Mu}^2 - 0.024h_{Mu} + 2.70, \quad (22)$$

$$\frac{Z_T}{Z} = 1.00 \times 10^{-4}h_{BC}^2 - 0.0436h_{BC} + 4.15. \quad (23)$$

These results suggest that, similarly to the case of BC/(SiC/SiC) interface, Z_T/Z for Mu/BC interface is dependent on the combination of the coating layer thicknesses in EBC.

The ERR for Mu/BC interface crack initiation in EBC is described as

$$G_{\text{Mu/BC}} = Z_{\text{Mu/BC}}(h_{\text{YbS}}, h_{\text{Mu}}, h_{\text{BC}}) \left(\frac{\sigma_{\text{YbS}}^2 h_{\text{YbS}}}{\bar{E}_{\text{YbS}}} + \frac{\sigma_{\text{Mu}}^2 h_{\text{Mu}}}{\bar{E}_{\text{Mu}}} \right), \bar{E}_i = \frac{E_i}{1 - \nu_i^2}, i = \text{YbS, Mu.} \quad (24)$$

Here, $Z_{\text{Mu/BC}}(h_{\text{YbS}}, h_{\text{Mu}}, h_{\text{BC}})$ is a factor dependent on the thicknesses of the layers in EBC.

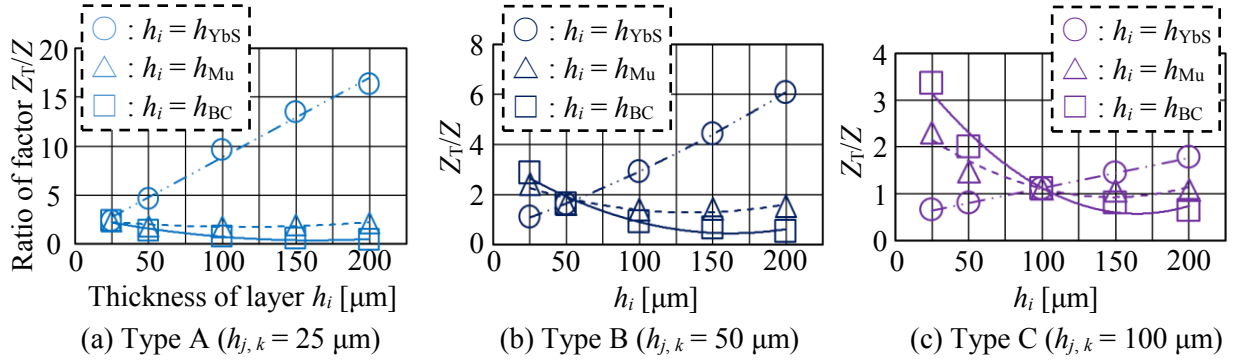


Fig. 3 Ratio of factor (Z_T/Z) for Mullite/Si-based bond coat interface – thickness of layers (h_i) relationships of (a) Type A, (b) Type B and (c) Type C.

4.1.3 Yb-silicate/Mullite interface. Figure 4 shows the Z_T/Z - h_i relationships for YbS/Mu interface. As well as the cases of BC/(SiC/SiC) and Mu/BC interfaces, (Z_T/Z)s of each type for YbS/Mu interface were changed by increasing the coating layer thicknesses. The relationships between Z_T/Z and h_i for YbS/Mu interfaces are written as

Type A

$$\frac{Z_T}{Z} = 0.0116h_{\text{YbS}} + 2.23, \quad (25)$$

$$\frac{Z_T}{Z} = 1.00 \times 10^{-4} h_{\text{Mu}}^2 - 0.0322h_{\text{Mu}} + 3.07, \quad (26)$$

Type B

$$\frac{Z_T}{Z} = 5.00 \times 10^{-5} h_{\text{YbS}}^2 + 3.00 \times 10^{-4} h_{\text{YbS}} + 3.00, \quad (27)$$

$$\frac{Z_T}{Z} = 3.00 \times 10^{-4} h_{\text{Mu}}^2 - 0.0945h_{\text{Mu}} + 7.70, \quad (28)$$

$$\frac{Z_T}{Z} = 0.0480h_{\text{BC}} + 1.06, \quad (29)$$

Type C

$$\frac{Z_T}{Z} = 3.00 \times 10^{-5} h_{\text{YbS}}^2 + 5.4 \times 10^{-3} h_{\text{YbS}} + 1.89, \quad (30)$$

$$\frac{Z_T}{Z} = 7.00 \times 10^{-4} h_{\text{Mu}}^2 - 0.226h_{\text{Mu}} + 19.3, \quad 50 \leq h_{\text{Mu}} \leq 200 \quad (31)$$

$$\frac{Z_T}{Z} = 0.0219h_{\text{BC}} + 0.597. \quad (32)$$

Here, the Z_T/Z - h_{BC} relationship of Type A cannot be defined in this analysis.

These equations indicate that the Z_T/Z - h_i relationship for YbS/Mu interface is also determined by the combination of the film thicknesses. Therefore, the theoretical equation of ERR for YbS/Mu interface crack initiation in EBC is modified as following equation:

$$G_{\text{YbS/Mu}} = Z_{\text{YbS/Mu}}(h_{\text{YbS}}, h_{\text{Mu}}, h_{\text{BC}}) \frac{\sigma_{\text{YbS}}^2 h_{\text{YbS}}}{\bar{E}_{\text{YbS}}}, \bar{E}_i = \frac{E_i}{1 - \nu_i^2}, i = \text{YbS} \quad (33)$$

Here, $Z_{YbS/Mu}(h_{YbS}, h_{Mu}, h_{BC})$ is a factor dependent on the thicknesses of the layers in EBC.

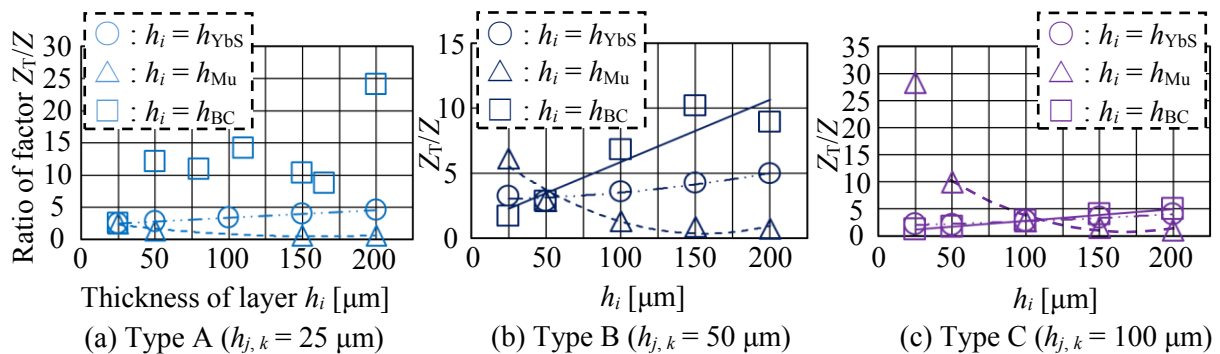


Fig. 4 Ratio of factor (Z_T/Z) for Yb-silicate/Mullite interface – thickness of layers (h_i) relationships of (a) Type A, (b) Type B and (c) Type C.

4.2. Condition of acceptable EBC layer thicknesses

Figures 5 (a) ~ (c) schematically show conditions on EBC layer thicknesses such that interface crack initiation is avoided for Type A. Following the Griffith theory, crack initiation occurs if ERR exceeds a critical value (G_c) determined by the interface fracture toughness. If Z in eq. (3) was a constant value (independent of layer thicknesses), ERR would be a linear function of thickness(es) of layer(s) above the interface in question. This means that there would be a plane that gives the critical layer thickness(es) and that the region surrounded by the plane and three axes would give acceptable layer thickness(es) to prevent interface crack initiation (see solid lines in Figs. 5 (a) ~ (c)). In fact, the shape of the region of acceptable EBC layer thicknesses becomes more complex because of the dependence of the factor on the layer thicknesses (eqs. (14), (24) and (33)), as is schematically shown as the hatched solids in Figs. 5 (a) ~ (c). Note that the region is depicted in a simple fashion; i.e., the actual shape of the boundaries between acceptable and unacceptable thicknesses may be complicated. The abovementioned $Z_T/Z-h_i$ relationships (eqs. (5) ~ (7), (15) ~ (17) and (25) ~ (26)) gives the actual shape.

As shown in Fig. 2 (a), Z_T/Z is greater than 1 ($G_T > G_F$) regardless of h_i . This means that the actual ERR is smaller than that estimated by eq. (3) with $Z = Z_T \equiv 1.028$. Thus, the condition on the coating layer thicknesses to prevent the BC/(SiC/SiC) interface crack initiation is loosened as indicated by the blue hatched area in Fig. 5 (a). On the other and, because Z_T/Z becomes smaller than 1 with the increase of h_{BC} as shown in Fig. 3 (a), the region of permissible layer thicknesses for Mu/BC interface is contracted as indicated by the green hatched area in Fig. 5 (b).

As shown in Fig. 5 (d), the region overlapped with the conditions for all interfaces gives permissible EBC layer thicknesses to prevent any interface crack initiation due to thermal stress during the fabrication process.

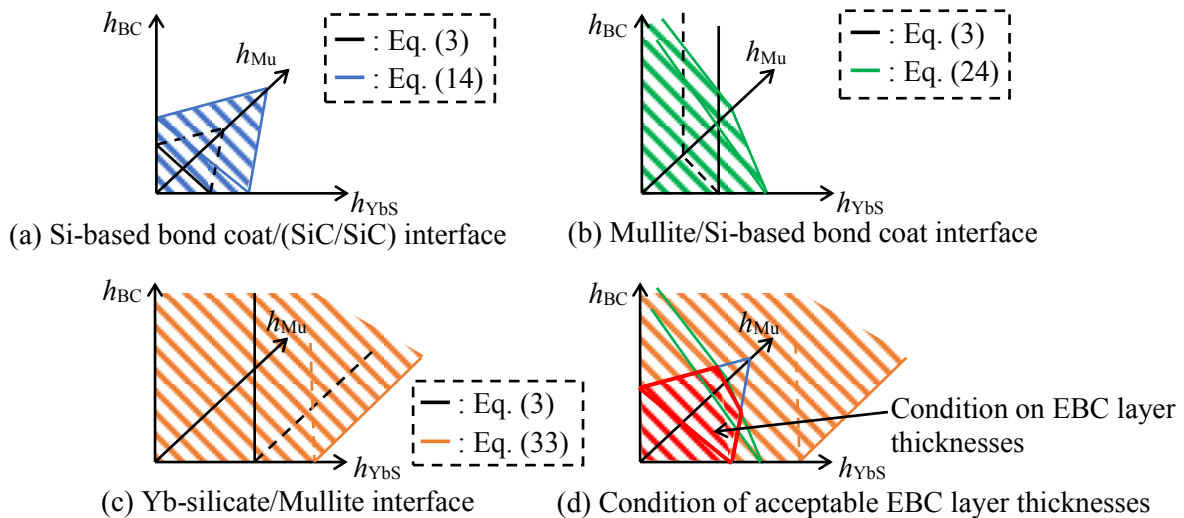


Fig. 5 Condition on EBC layer thicknesses for Type A to prevent the (a) Si-based bond coat/(SiC/SiC) interface, (b) Mullite/Si-based bond coat interface, (c) Yb-silicate/Mullite interface crack initiation due to thermal stress during fabrication process and (d) condition of acceptable EBC layer thicknesses for Type A which is obtained by superposing (a) ~ (c).

5. Conclusion

To establish theoretical prediction for acceptable EBC layer thicknesses that ensure the mechanical reliability of EBC, we conducted FEM analysis to calculate ERRs for interface crack initiation due to thermal stress in EBC. The results were compared with a simple theory for interface crack in a single-layered structure where ERR is estimated as nominal strain energy in the coating layers multiplied by a constant factor. It was shown that the factor is no longer a constant but depends on layer thicknesses in EBC. We obtained the factor as a function of EBC layer thicknesses and presented condition of EBC layer thicknesses based on the results.

References

- [1] David L M, Tito T S and James A D, 1986, *J.Mater.Eng*, **8** 1, 80-91
- [2] Anand A and Alta Y N C, 1997, *J.Mater.Process.Tech.*, **63**, 384-94
- [3] Joosung J L, Stephen P L, Ian A W and Andreas S, 2001, *Annu.Rev.Energy Environ*, **26**, 167-200
- [4] Irene S and Jim S, 2004, *Int.J.Appl.Ceram.Technol*, **1** 4, 291-301
- [5] Tresa M P and Sammy T, 2006, *J.Propul.Power*, **22** 2, 361-74
- [6] Kang N L and Robert A M, 1996, *Surf.Coat.Tech.*, **86-87**, 142-8
- [7] Sivakumar R, Surendra N T, Kang N L, Ramakrishna T B and Dennis S F, 2011, *Surf.Coat.Tech.*, **205**, 3578-81
- [8] John W H and Zhigang S 1991 *Advances in Applied Mechanics* vol 29 ed John W H and Theodore Y Wu (Amsterdam: Elsevier) pp 63-191

Acknowledgment

This work was supported by Council for Science, Technology and Innovation (CSTI), Cross-ministerial Strategic Innovation Promotion Program (SIP), "Structural Materials for Innovation" (Funding agency: JST, Japan Science and Technology Agency).